Chinese Journal of Aeronautics, (2014),27(2): 272–279

Chinese Society of Aeronautics and Astronautics
& Beihang University

Chinese Journal of Aeronautics

cja@buaa.edu.cn
www.sciencedirect.com

Study of parachute inflation process using fluid–structure interaction method

Yu Li *, Cheng Han, Zhan Ya'nan, Li Shaoteng

College of Aerospace Engineering, Nanjing University of Aeronautics and Astronautics, Nanjing 210016, China

Received 25 March 2013; revised 28 August 2013; accepted 11 October 2013
Available online 28 February 2014

KEYWORDS

Empirical formula;
Fluid–structure interaction;
Inflation process;
Opening shock;
Parachute;
Wind tunnel test

Abstract A direct numerical modeling method for parachute is proposed firstly, and a model for the star-shaped folded parachute with detailed structures is established. The simplified arbitrary Lagrangian–Eulerian fluid–structure interaction (SALE/FSI) method is used to simulate the inflation process of a folded parachute, and the flow field calculation is mainly based on operator splitting technique. By using this method, the dynamic variations of related parameters such as flow field and structure are obtained, and the load jump appearing at the end of initial inflation stage is captured. Numerical results including opening load, drag characteristics, swinging angle, etc. are well consistent with wind tunnel tests. In addition, this coupled method can get more space–time detailed information such as geometry shape, structure, motion, and flow field. Compared with previous inflation time method, this method is a completely theoretical analysis approach without relying on empirical coefficients, which can provide a reference for material selection, performance optimization during parachute design.

1. Introduction

Phenomena such as canopy collapse or contraction, apex whipping, asymmetric inflation, etc. usually occur because of the fluid–structure interaction during parachute inflation process.[1] The inflation process is transient and shorter than 1 s in most situations, making it difficult to measure the time-sequence canopy shape, the flow field and other dynamic data. Therefore, the experimental study on the parachute inflation process mostly focuses on the opening shock load which can be easily measured.[2–5] From 2006, earlier studies on the dynamic relationship between the projected diameter and opening shock of a flat circular parachute were published, in which high speed camera and dynamic balance were used based on synchronous measure technology.[4,5] However, the corresponding literature on the dynamic relationship between the fluid field and structure in inflating is still unavailable.

The fluid–structure interaction (FSI) problem of parachute is highly nonlinear and unsteady, which is very difficult and complex. Therefore the earlier numerical studies focused on the dynamics of the parachute and payload system, which need to rely on empirical formula or data. The typical methods are inflation distance method, inflation time method, radical momentum equation method, etc.[6,7] All of those methods need

* Corresponding author. Tel.: +86 25 84893739.
E-mail address: yuli_happy@163.com (L. Yu).

Peer review under responsibility of Editorial Committee of CJA.

1000-9361
http://dx.doi.org/10.1016/j.cja.2014.02.021

to be based on drag characteristics and associated air mass experience formulas which are summed from experiments. The parachute–payload system is divided into several objects described by particle or rigid body in those methods. And the trajectory, load and other parameters of research objects may be obtained, but the canopy shape and stress, the flow field surrounding the parachute and other dynamic characteristic cannot be obtained. The fluid–structure interaction mechanical mechanisms of the parachute during the inflation stage can't be revealed.

With the continuous development of numerical algorithms and the computer hardware, FSI problem of parachute has been attracting scholars' attention at home and aboard. The computational fluid dynamics/mass spring damper (CFD/MSD) model is used in the earlier FSI method based on time–space dispersing. In this model, the parachute is dispersed into a series of mass points connected by the springs and dampers. And their movement is controlled by flow field force, spring force and damping force.[8–10] The first application of parachute based on this method can be found in Ref.[8] and in that work the inflating process of the 2D axial symmetry round parachute surrounded by flow field was calculated. This method focuses on the canopy shape calculation, but the stress distribution of the canopy cannot be obtained. At present, one of the most commonly methods is the deforming-spatial-domain/stabilized space–time (DSD/SST) coupling method, which can obtain the detailed description of the flow field and structure during the parachute inflation process. This is an interface tracking method aiming to solve the large deformation in coupling calculation, which was proposed in the 1990s.[11,12] In DSD/SST method, both flow field and structure are dispersed by a large number of elements. The time–space FSI problem was solved using dynamic grid technology. The method was firstly used in Ref.[13] for 2D computation of the flat circle parachute during the inflation process. The same method was also used in 3D FSI calculation of parafoil, circular parachute, cross parachute and ringsail parachute.[14–19] The initial unfolded shape was greatly simplified in those works. Besides the DSD/SST technology, the immersed boundary (IB) method was used to solve the FSI simulation problems of parachute inflating, and this method was used in simulating the cone parachute and cluster parachute.[20] These methods mentioned above are based on Navier–Stokes equations, while the other method, such as large eddy simulation method, was used for FSI simulation of disk-gap-band parachute in supersonic flow field in Ref.[21] In recent years, studies of the three-dimensional FSI problem of the parachute based on the business software LS-DYNA also made great progress.[22–24] The FSI calculation on the quasi-inflation process of the slotting circular parachute, rectangular parachute and crucial parachute was studied in Refs.[23,24], and the initial shape was supposed to be a spreading shape. The same method is also used in simulating the inflation process of flat circular parachute and bottom-stretching parachute in Refs.[22,24], in which the structural details of parachute such as radial and zonal band were ignored. The initial structural model of the parachute obtained by calculation is called load hung method. The canopy model will move from a fattened state to a folded state when the tension load was applied to some nodes. If the parachute is made from many types of materials or the structure is complex, the initial grid of canopy will be distorted and the calculation will become more complex.

Most previous research works of parachute inflation using the space–time FSI technique are based on a supposed initial canopy shape and the structure details are ignored. In this work, the folded canopy model including the structure details was established by direct folding method, which is simple and easy to realize. Based on this direct modeling, the folded ringslot inflating is simulated by SALE/FSI method for the first time. Based on the SALE method, the 3D FSI computation of a folded ringslot inflating was realized. The accuracy and efficiency of the simulation results in this work are also verified by the experimental data. In this method, more space–time details such as flow field, stress, canopy shape and other characteristics can be obtained compared with the traditional dynamics method of parachute–payload system.

This coupling calculation was carried out by the DELL T5500 workstation with 12-core, 32 G memory. The CPU time consumption of which was about 145 h.

2. Mathematical model

2.1. Control equation of fluid field

At the inflation stage of the flexible canopy, the flow field grids near the structure will produce large deformation. In order to avoid serious distortion of the calculation grids, the simplified arbitrary Lagrange–Euler (SALE) method is used to calculate the inflation stage of the parachute.

The control equations of flow field are as follows:

$$\begin{cases} \dfrac{\partial \rho}{\partial t} + \rho \dfrac{\partial v_i}{\partial x_i} + c_i \dfrac{\partial \rho}{\partial x_i} = 0 \\ \rho \dfrac{\partial v_i}{\partial t} + \rho c_i \dfrac{\partial v_i}{\partial x_j} = \sigma_{ij,j} + \rho b_i \\ i,j = 1,2,3 \end{cases} \tag{1}$$

where ρ is the density, t the time, v_i the velocity, x_i the Eulerian coordinate, c_i the relative velocity in reference field, b_i the body force; stress $\sigma_{ij} = -p\delta_{ij} + \mu(v_{i,j} + v_{j,i})$, p is the pressure, μ the viscosity, δ_{ij} the Kronecker coefficient.

Initial conditions: $\boldsymbol{v}_{\mathrm{F}}^0 = \boldsymbol{v}_{\mathrm{inlet}}$, $p_{\mathrm{F}}^0 = 101325$ Pa, the superscript "0" means the initial time. Boundary conditions of the calculation field: inlet boundary, $\boldsymbol{v}_{\mathrm{inlet}} = \overline{\boldsymbol{v}}$; outlet boundary, $\dfrac{\partial p_{\mathrm{F}}}{\partial n} = 0$, $\dfrac{\partial \boldsymbol{v}_{\mathrm{F}}}{\partial n} = 0$; the around boundary, $\dfrac{\partial \boldsymbol{v}_{\mathrm{F}}}{\partial n} = 0$.

2.2. Structure control equation

The control equation of the structure calculation (coupling faces) is as follows:

$$\rho_{\mathrm{S}} \frac{\mathrm{d}^2 u_i}{\mathrm{d}t^2} = \sigma_{ij,j} + \rho_{\mathrm{S}} b_i \tag{2}$$

Initial conditions: $\boldsymbol{v}_{\mathrm{S}}^0 = 0$, $\boldsymbol{\sigma}_{\mathrm{S}}^0 = 0$. Boundary condition of the lines intersection: $\boldsymbol{u}_{\mathrm{S}} = \boldsymbol{0}$.

When the canopy elements contact each other, the contact force $\boldsymbol{F} = k\boldsymbol{d}$ is exerted. The penalty function coefficient k is affected by the distance of coupling point $\boldsymbol{d}$ and stiffness coefficient of fabric. Penalty method based on Ergun equation is also used for the realization of FSI.

3. Numerical arithmetic

In the actual wind tunnel experiment, the intersection of lines is fixed. Therefore the change of flow field computational do-

main is limited. In order to simulate the conical ringslot inflating in this state, the referenced grid of flow field in SALE/FSI method can be fixed in this state.

The parachute structure simulation method is mainly based on Lagrangian arithmetic. The calculation grids are fixed on the structure and move with the material. Thus the information of mobile boundary of the parachute can be described accurately.

The inlet velocity is constant and set as 18 m/s in the infinite mass state of parachute inflation process. The SALE/FSI method is processed to solve the serious distorted flow field grids during calculation. The flow field calculation is mainly based on splitting technique. For each step forward in time, there are three distinct sub-steps: (A) solving the flow field based on Lagrangian arithmetic, and getting state parameters in Lagrangian coordinate; (B) smoothing the distorted fluid material grids based on "Equipotential" zoning method, in which the topology relationship of grids does not change; (C) transporting the flow field information to the updated grids based on advection methods. These sub-steps are shown in Fig. 1. At the end of Step (C), the solution is prepared for the next time step.

3.1. The Lagrangian arithmetic

In the Sub-step (A), the grids move with the material deformation. Therefore the convective terms and the mass equation in the governing Eq. (1) can be ignored. The control equation of the flow field and structure can be simplified as follows:

$$M\ddot{u}_i + F_i^{\text{int}} = F_i^{\text{ext}} \quad (i = 1, 2, 3) \tag{3}$$

where, the three terms stand for inertia force, internal force and external force respectively from left to right, M is the mass and $\ddot{u}_i$ the acceleration.

The nodal displacement is calculated based on the discrete Eq. (3) by using finite element method (FEM). After calculating the nodal acceleration, centered-differences are used to find the velocity at time $n + 1/2$, and the new position of the node at time level $n + 1$, n is the time step.

Then the stress, strain and other parameters of elements can be got at time $n + 1$. In general, the time step Δt must be chosen small enough to guarantee calculation stability. In this paper, the time step is chosen as follows:

$$\Delta t < \Delta t_c = \alpha(L_{\min}/c) \tag{4}$$

where $L_{\min}$, c, α stands for the minimum cell size, sonic speed of the material and zooming factor respectively ($\alpha = 0.7$ in this work).

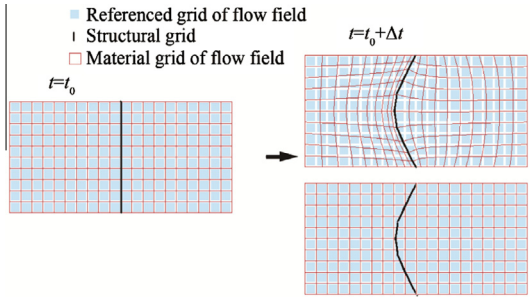

Fig. 1 Operation of each time step.

3.2. Smoothing grids

In this work, the inlet velocity is constant and the referenced grids of the flow field are fixed during parachute inflation. After the Lagrangian time step calculation of the flow field is carried out, the fluid material grids will be distorted. Thus they must be smoothed by equipotential method which was developed by Winslow[25] in order to guarantee the grid quality. Equipotential zoning is a method to establish a structured mesh for finite difference or finite element calculations by solving the Laplace equations (later extended to Poisson equation). The topological relation of the smoothed mesh is the same as the original one. The new nodal position of mesh is determined by the following equation based on equipotential arithmetic:

$$\alpha_1\partial_{\xi_1\xi_1}\boldsymbol{x} + \alpha_2\partial_{\xi_2\xi_2}\boldsymbol{x} + \alpha_3\partial_{\xi_3\xi_3}\boldsymbol{x} + 2\beta_1\partial_{\xi_1\xi_2}\boldsymbol{x} + 2\beta_2\partial_{\xi_1\xi_3}\boldsymbol{x} + 2\beta_3\partial_{\xi_2\xi_3}\boldsymbol{x} = \boldsymbol{0}$$

where

$$\alpha_i = \partial_{\xi_i}x_1^2 + \partial_{\xi_i}x_2^2 + \partial_{\xi_i}x_3^2$$
$$\beta_1 = (\partial_{\xi_1}\boldsymbol{x}\cdot\partial_{\xi_3}\boldsymbol{x})(\partial_{\xi_2}\boldsymbol{x}\cdot\partial_{\xi_3}\boldsymbol{x}) - (\partial_{\xi_1}\boldsymbol{x}\cdot\partial_{\xi_2}\boldsymbol{x})\partial_{\xi_3}\boldsymbol{x}^2$$
$$\beta_2 = (\partial_{\xi_2}\boldsymbol{x}\cdot\partial_{\xi_1}\boldsymbol{x})(\partial_{\xi_3}\boldsymbol{x}\cdot\partial_{\xi_1}\boldsymbol{x}) - (\partial_{\xi_2}\boldsymbol{x}\cdot\partial_{\xi_3}\boldsymbol{x})\partial_{\xi_1}\boldsymbol{x}^2$$
$$\beta_3 = (\partial_{\xi_3}\boldsymbol{x}\cdot\partial_{\xi_2}\boldsymbol{x})(\partial_{\xi_1}\boldsymbol{x}\cdot\partial_{\xi_2}\boldsymbol{x}) - (\partial_{\xi_3}\boldsymbol{x}\cdot\partial_{\xi_1}\boldsymbol{x})\partial_{\xi_2}\boldsymbol{x}^2$$

In order to obtain more even mesh, the Simple Averaging arithmetic is also used. The coordinates of a node are the simple average of the coordinates of its surrounding nodes as follows:

$$\boldsymbol{x}_{\text{SA}}^{n+1} = \frac{1}{N}\sum_{i=1}^{N}\boldsymbol{x}_i^n \tag{6}$$

A composite algorithm is generated using a weighted average of those two algorithms above, where the subscripts "E" and "SA" refers to the equipotential and simple averaging algorithm respectively, and w is the weighting factor.

$$\boldsymbol{x}^{n+1} = w_{\text{E}}\boldsymbol{x}_{\text{E}}^{n+1} + w_{\text{SA}}\boldsymbol{x}_{\text{SA}}^{n+1} \tag{7}$$

3.3. Advection algorithms

As a fluid element moves from its position at the end of the Lagrange calculation to its new position after mesh smoothing, there are mass, momentum and energy flux through the six faces of the element. Since advection is merely a geometric update of the mesh, the source terms of the governing equation disappear. The advection equation can be described as follows:

$$\frac{\partial\phi}{\partial t} + \frac{\partial c_i\phi}{\partial x_i} = 0 \tag{8}$$

where ϕ is the generalized variable.

As for the three-dimensional problem, the convection term is discrete which is expressed by the following common form:

$$\phi_{\text{A}}^{n+1}V_{\text{A}}^{n+1} = \phi_{\text{A}}^{n}V_{\text{A}}^{n} + \sum_{j=1}^{6}f_j^{\phi} \tag{9}$$

$$\begin{cases} f_j^{\phi} = \dfrac{c_j}{2}(\phi_j^- + \phi_j^+) + \dfrac{|c_j|}{2}(\phi_j^- - \phi_j^+) \\ \phi_j^+ = S_{j+\frac{1}{2}}^n(x_j^n + \frac{1}{2}\Delta t c_j - x_{j+\frac{1}{2}}^n) + \phi_{j+\frac{1}{2}}^n \\ \phi_j^- = S_{j-\frac{1}{2}}^n(x_j^n + \frac{1}{2}\Delta t c_j - x_{j-\frac{1}{2}}^n) + \phi_{j-\frac{1}{2}}^n \end{cases} \tag{10}$$

Table 1 Parameters of textile material.

Structure	Density (g/m^3)	Thickness/diameter (mm)	Poisson ratio	Width (mm)	Young's modulus (Pa)
Canopy	130	0.03	0.14		5.87×10^9
Suspension	7	2.5			6.52×10^8
Reinforcement belt	5	0.1		15	3.42×10^9

$$\begin{cases} S^n_{j+\frac{1}{2}} = \dfrac{\left(\phi^n_{j+\frac{3}{2}} - \phi^n_{j+\frac{1}{2}}\right)\Delta x_j^2 + \left(\phi^n_{j+\frac{1}{2}} - \phi^n_{j-\frac{1}{2}}\right)\Delta x_{j+1}^2}{\Delta x_j \Delta x_{j+1}\left(\Delta x_j + \Delta x_{j+1}\right)} \\ \Delta x_j = x^n_{j+\frac{1}{2}} - x^n_{j-\frac{1}{2}} \\ \Delta x_{j+1} = x^n_{j+\frac{3}{2}} - x^n_{j+\frac{1}{2}} \end{cases} \tag{11}$$

where, the expression of $S^n_{j-\frac{1}{2}}$ is the same as Eq. (11). The subscript "j" refers to calculation element and its surrounding element respectively. V is element volume. The value of f_j^{ϕ} depends on the velocity at node j, which defines the upstream direction. The staggered mesh algorithm and monotone upwind schemes for conservation laws (MUSCL) scheme with the second order precision are applied to calculating the flux of mass, momentum and energy through the element faces.

4. Structure and numerical model

4.1. Parameters of the parachute

A kind of conical ringslot is involved in this work. The parachute is made up of 20 gores and 5 rings. The textile fiber materials of the canopy, suspension, and reinforcement line are brocade silk, aramid and brocade silk respectively. And the material parameters are shown in Table 1. The symmetrical section of the ringslot from a top view is shown in Fig. 2, in which the AA' is the symmetrical line, the apex angle is 16.9°, the vent diameter is 0.54 m, the nominal area is 30 m^2, and suspension length is 7.4 m.

4.2. Finite element model

The direct folding modeling technology[26,27] was applied to establishing the initial finite element model of parachute with completely straightened suspensions. The canopy looks like "*" from overlooking (see Fig. 3). The direct folding modeling method is simple and does not need calculation compared with load hung method. Therefore more structure details including reinforce belt, geometric porosity, etc. can be described. Moreover, the folded extent and the initial inlet area can be adjusted conveniently. In this work, the folded angel of the canopy is only 1° and the initial inlet area is just 0.085 m^2. The direct folding method also makes it convenient to program and to establish folded numerical model. The canopy is meshed by 36200 triangular elements. The suspension and reinforcement belt are meshed by bar elements with 4760 nodes. The hexahedral elements are used to mesh the flow field, and flow field grids are over 690000. The computational domain along the axial, radical and zonal is $10D_0\times5D_0\times5D_0$ respectively (D_0 is the nominal diameter, and the length of wake flow is about $6D_0$). The initial element model of the flow field and parachute is shown in Fig. 4.

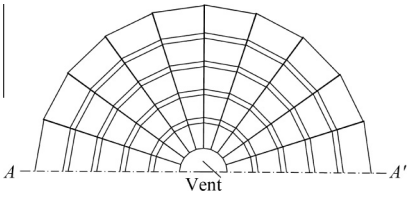

Fig. 2 Top view of conical ringslot model (half).

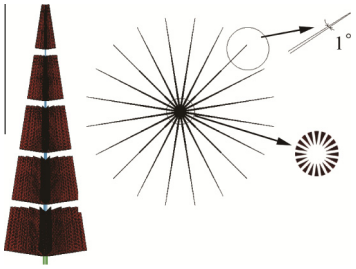

Fig. 3 Initial model of parachute.

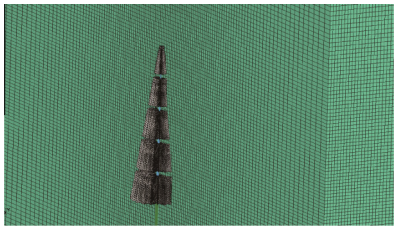

Fig. 4 Initial grid of parachute and flow field.

5. Numerical results and discussion

5.1. Flow field and shape of the structure

Fig. 5 shows the time-sequence results of coupling calculation such as the canopy shape change including stress contour, pressure and velocity of the flow field in a symmetrical section. The following conclusions can be obtained according to the numerical results.

(1) The canopy skirt opens first, and then the canopy inflates from apex to skirt, which reflect the influence of airflow entered into the canopy. The space–time change of canopy stress is also decided by the space–time deformation of canopy. The canopy is not completely symmetric inflated because of the asymmetric flow (see Fig. 5).

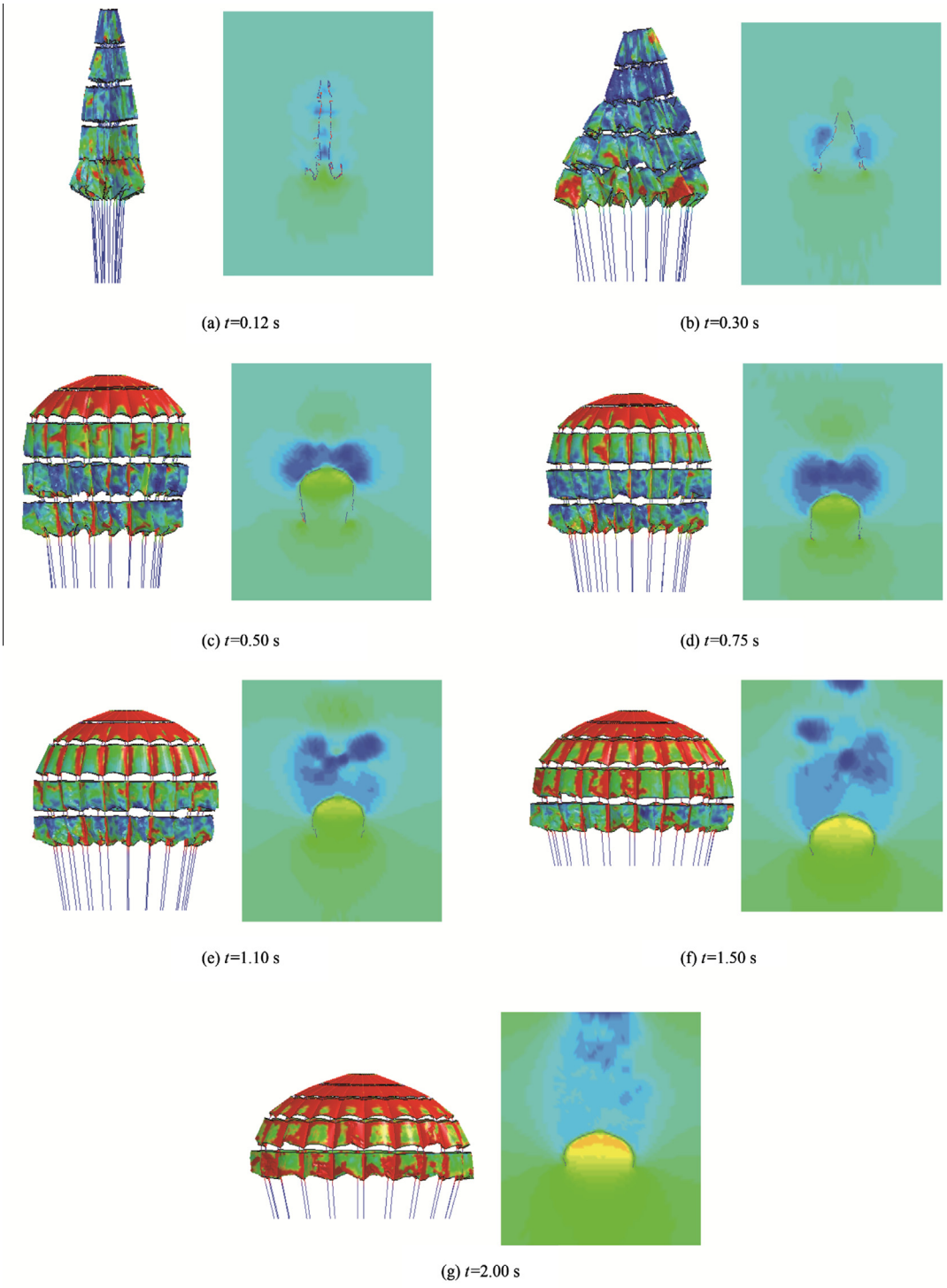

Fig. 5 Structure and flow field of time-sequence during inflation process (left: canopy shape with stress contour; right: pressure contour).

(2) During the inflation process, the maximum effective stress appears at the initial inflation phase, the 0.42 s. The position is at the middle part of the second ring which departs form the apex at about one-third of the radius length. The canopy will not be damaged even with the maximum effective stress (1.907×10^8 Pa).
(3) At the initial inflation stage, each seam between rings can be an assistant inlet and accelerate the inflation, and the velocity and pressure distribution of flow field around which is similar. At the main inflation stage, each seam works as the outlet to reduce the opening shock and inflation speed of the canopy with the increasing internal pressure (see Fig. 5(b) and (c)).
(4) The wake vortex begins to develop near the canopy surface at first. Then it moves downstream, and at the meantime, becomes bigger and longer. Finally, the vortex breaks into pieces and moves far away (see Fig. 5(b) and (c)).

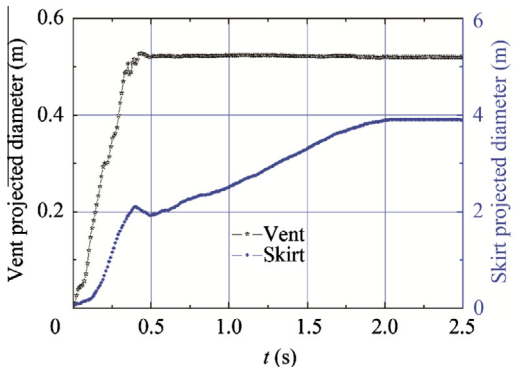

Fig. 6 Numerical results of projected diameter.

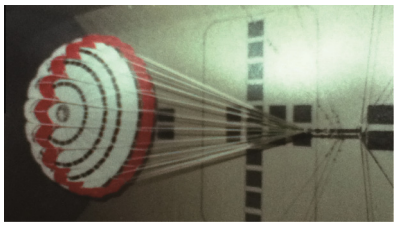

Fig. 7 Wind tunnel test.

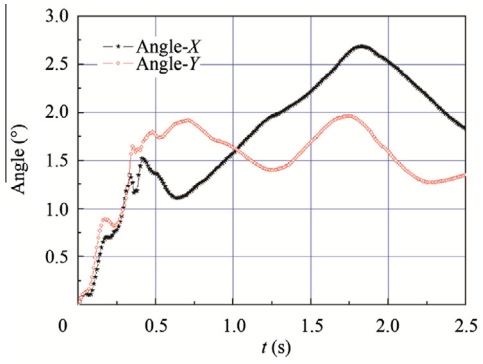

Fig. 8 Swinging of the parachute during inflation process.

5.2. Inflation time and the projected diameter

In Fig. 6, the evenly projected diameter of the vent and skirt is 0.52 m and 3.90 m at terminal stage respectively. The ratio of the inlet projected diameter and nominal diameter is 0.63. It is consistent with the statistical data which ranges from 0.60 to 0.65.[7] The start time of the vent opening and skirt opening is defined as the initial inflation time and fully inflated time respectively. Then the initial inflation time and the fully inflated time are 0.46 s and 2.00 s, which are shorter than the ones in wind tunnel experiment (0.58 s and 2.17 s respectively). The canopy is soft, light and large, and the inflation status of parachute is greatly influenced by air flow, package manner, manufacturing process of parachute and other factors. In the actual situation, which is not the ideal state, the canopy inflation is usually asymmetrical but not synchronized. Therefore the inflation time will be prolonged significantly in tests. In short, the numerical results such as inflation time and projected diameter can satisfy the demand of engineering analysis.

5.3. Swinging

A wind tunnel test was carried out and its state was set the same as the calculation state (see Fig. 7). The force balance was used to measure parachute opening shock load, and the binocular camera method was used to obtain the canopy swinging change. According to definition of Descartes's coordinate system, the vertical, horizontal and the central axis direction of the parachute is defined as X, Y, Z coordinate directions respectively. Numerical calculation results of swinging are shown in Fig. 8 and the results comparison of numerical simulation and experiment is shown in Table 2. The experimental swinging angle is slightly bigger because it is difficult to keep the flow field in wind tunnel absolutely symmetric and the canopy structure is also not symmetric due to the manufacturing process and design. However, the numerical swinging angle is consistent with the result of wind tunnel test, and both results show that this parachute has good stability.

5.4. Opening shock and drag characteristics

It can be found that the numerical results of drag area and opening shock are consistent well with the wind tunnel test data in Table 2. The drag area and opening load of the inflation process are shown in Figs. 9 and 10. Moreover, Fig. 10 shows the experience formula which is based on the inflation time method.[7] The results show that:

(1) During the same parachute inflation state, the change of opening load is similar to the drag area, but this correlation is nonlinear. Because the opening shock of parachute is not only related to drag area but also related to the change rate of drag area.
(2) Both the maximum load and maximum drag area occur at the time when the canopy is completely open, which follows the change regulation of inflation process in infinite mass condition. Both results based on FSI method and experimental method appear the first opening load peak at the time when the vent is completely open (about at 0.50 s). But this phenomenon cannot be reflected by inflation time method.

Table 2 Results comparison of numerical simulation and experiment.

Value	Vertical maximum swinging angle (°)	Horizontal maximum swinging angle (°)	Drag area at fully inflated state (m^2)	Opening shock (N)
Test	3.13	3.09	18.2	3724
Calculation	2.69	2.01	18.4	3890

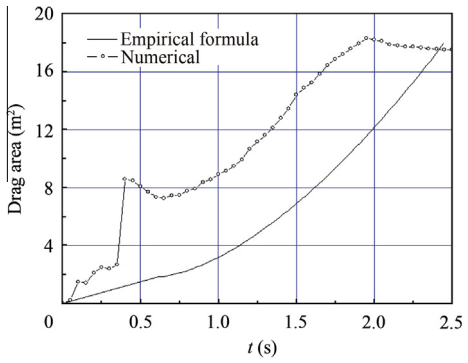

Fig. 9 Drag area of ringslot.

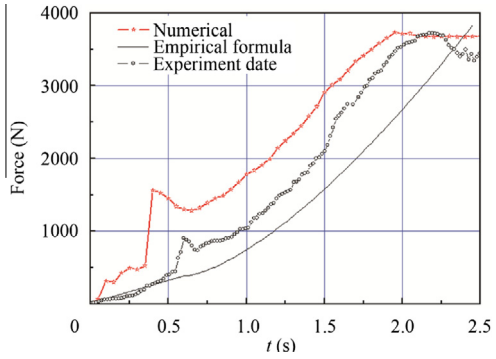

Fig. 10 Opening load of ringslot.

Affected by the preceding air flow peak, the canopy opens gradually from bottom to apex. The flexible canopy has light mass and cannot support the bending. Therefore, at the initial inflation stage, the upper folded part of the canopy will produce some second folding due to its swinging and twisting aroused by the fluid force and structural force. This may cause the parachute opening to be difficult. When the apex is completely open the second folding disappears rapidly, and the opening load will jump because of the rapid growth of deploy area. Therefore the first opening shock is influenced by the second folding of the upper canopy. The first opening shock appearing at initial inflation stage reflected by numerical simulation or experimental method reveals the interaction mechanism of flow field and structure, which is consistent with the actual situation. However, the time-sequence drag area is assumed continuous and smooth by the inflation time method,[7] which does not agree with the practical situation. Moreover, the empirical coefficient selected may not be appropriate for the specified geometric dimension of parachute or specified working state.

6. Conclusion

In this paper, the direct folding method is applied to establishing the initial folded parachute model and shows that: (A) this method is convenient in modeling the structure details; (B) the application is simple without calculation compared with the load hung method; (C) it is easy to adjust the folding rate and inlet area. Then, the space–time FSI technique based on SALE method is used to simulate the parachute inflation process and is proven to be able to solve the large deformation problem of parachute. The numerical results are in good agreement with the test data, which shows that this method has high accuracy. Moreover, it can provide more space–time fluid–structure–motion information such as the canopy shape, the opening shock, swinging, etc. compared with the empirical method, and can better reveals the mechanical mechanism of parachute inflation process. All the results show that the space–time SALE method is recommendable in numerical simulation of parachute FSI problem and can satisfy the following purposes:

(1) Predicting time-sequence change of the canopy shape with stress and providing reference for the material selection and structure optimization.
(2) Predicting aerodynamic characteristics of parachute and providing reference for the payload–parachute system design and trajectory study.
(3) Predicting the swinging and stability of the parachute and taking further researches on the stability and twine problems of the payload–parachute system.

In a word, the FSI method of the parachute inflation process is a complete theoretical method which does not depend on empirical coefficient. Based on this method, the interactive mechanical mechanism of fluid force and structural force during parachute working can be revealed and more space–time information of fluid–structure–motion can be obtained.

Acknowledgments

The authors are grateful to Yan Xiaoxue for her careful polishing. This study was co-supported by the National Natural Science Foundation of China (No. 11172137) and the Aeronautical Science Foundation of China (No. 20122910001).

References

1. Orlik-Rueckemann KJ, Maydew RC, Peterson CW. Design and testing of high-performance parachutes. NASA-ADA-246343; 1992.
2. Wolf N, Whitmore T, Jensen S. Design and testing of collapsible drogue parachute for the X-37 Vehil. AIAA-2005-1660; 2005.
3. Jason PS, Hart A. Canned telemetry system for sensor data on parachute system. AIAA-2005-1513; 2005.
4. Yu L, Ming X, Hu B. Experimental investigation in parachute opening process. *J Nanjing Univ Aeronaut Astronaut* 2006;**38**(2):176–80 [Chinese].
5. Yu L, Zhang XH, Li SS. Experimental on canopy payload performance of parachute. *J Beijing Univ Aeronaut Astronaut* 2007;**33**(10):1178–81 [Chinese].
6. Peng Y, Zhang QB, Cheng WK. Summary for the research methods of parachute inflation process. *Chin Space Sci Technol* 2003;7–12 [Chinese].
7. Wang LR. *Parachute theory and applications*. Beijing: Aerospace Press; 1997. p. 187–229.
8. Stein KR, Benney RJ, Steeves EC. A computational model that couples aerodynamic structural dynamic behavior of parachutes during the opening process. NASA-ADA-264115; 1993.
9. Yu L, Ming X. Study on transient aerodynamic characteristics of parachute opening process. *Acta Mech Sin* 2007;**23**(6):627–33 [Chinese].

10. Yu L, Shi XL, Ming X. Numerical simulation of parachute during opening process. *Acta Aeronaut Astronaut Sin* 2007;**28**(1):52–7 [Chinese].
11. Tezduyar TE, Behr M, Mittal S. A new strategy for finite element computations involving moving boundaries and interfaces—the deforming-spatial-domain/space–time procedure: I. The concept and the preliminary numerical tests. *Comput Methods Appl Mech Eng* 1992;**94**(3):339–51.
12. Tezduyar TE, Behr M, Mittal S. A new strategy for finite element computations involving moving boundaries and interfaces—the deforming-spatial-domain/space–time procedure: II. Computation of free-surface flows, two-liquid flows, and flows with drifting cylinders. *Comput Methods Appl Mech Eng* 1992;**94**(3):353–71.
13. Stein KR, Benney RJ, Kalro V, Johnson AA, Tezduyar TE. Parallel computation of parachute fluid–structure interactions. AIAA-1997-1505; 1997.
14. Kalro V, Tezduyar T. A parallel 3D computational method for fluid–structure interactions in parachute systems. *Comput Methods Appl Mech Eng* 2000;**190**(3–4):321–32.
15. Stein K, Benney R, Kalro V, Tezduyar TE, Leonard J, Accorsi M. Parachute fluid–structure interactions: 3-D Computation. *Comput Methods Appl Mech Eng* 2000;**190**(3):373–86.
16. Stein K, Benney R, Tezduyar T. Fluid–structure interaction of a cross parachute: numerical simulation. *Comput Methods Appl Mech Eng* 2001;**191**(6–7):673–87.
17. Tezduyar TE, Sathe S, Pausewang J, Schwaab M, Christopher J, Crabtree J. Fluid–structure interaction modeling of ringsail parachutes. *Comput Mech* 2008;**43**(1):133–42.
18. Takizawa K, Wright S, Moorman C, Tezduyar TE. Fluid–structure interaction modeling of parachute clusters. *Int J Numer Methods Fluids* 2011;**65**(1–3):286–307.
19. Kenji T. Fluid structure interaction modeling of spacecraft parachutes for simulation-based design. *J Appl Mech* 2012;**79**(1):1–9.
20. Kim YS, Peskin CS. 3-D parachute simulation by the immersed boundary method. *Comput Fluids* 2009;**38**(6):1080–90.
21. Karagiozis K, Kamakoti R, Cirak F, Pantano C. A computational study of supersonic disk-gap-band parachutes using Large-Eddy simulation coupled to a structural membrane. *J Fluids Struct* 2011;**27**(2):175–92.
22. Tutt BA, Taylor AP. The use of LS-DYNA to simulate the inflation of a parachute canopy. AIAA-2005-1608; 2005.
23. Tutt BA, Taylor AP, Jean CB, Gargano B. The use of LS-DYNA to assess the performance of airborne systems North America candidate ATPS main parachutes. AIAA-2005-1609; 2005.
24. Coquet Y, Bordenave P. Improvements in fluid structure interaction simulation of parachute using LS-Dyna. AIAA-2011-2590; 2011.
25. Winslow AM. Numerical solution of the quasilinear Poisson equation in a nonuniform triangle mesh. *J Comput Phys* 1997;**135**(2):128–38.
26. Ma CS, Yue H, Huang SL. A study on airbag folding patterns for improving occupant protection effectiveness. *Automot Eng* 2005;**27**(3):350–3.
27. Cheng H, Yu L, Yin ZW. A new method of complicated folded fabric modeling. *J Harbin Inst Technol* 2012;**19**(2):43–7.

Yu Li received Ph.D. degree from Nanjing University of Aeronautics and Astronautics (NUAA) in 2006. Now, she is a professor and doctoral tutor in College of Aerospace Engineering, NUAA. Her main research interests are fluid structure interaction, ADS design, and environmental control systems.